Helical Polyacetylenes Synthesized in Helical Sense and Pitch Controllable Chiral Nematic Liquid Crystal with Unprecedented Temperature Dependence

Munju Goh,[†] Takayuki Matsushita,[‡] Mutsumasa Kyotani,[§] and Kazuo Akagi*,[†]

Department of Polymer Chemistry, Kyoto University, Katsura, Kyoto 615-8510, Japan; Institute of Materials Science, University of Tsukuba, Ibaraki 305-8573, Japan; and Tsukuba Research Center for Interdisciplinary Materials Science (TIMS), University of Tsukuba, Ibaraki 305-8573, Japan

Received February 12, 2007; Revised Manuscript Received May 16, 2007

ABSTRACT: We have synthesized two types of novel chiral compounds, D-1 and D-2−D-5, where D-1 is an asymmetric center-containing chiral compound of (*S*)-configuration, and D-2−D-5 are so-called double chiral compounds consisting of axially chiral binaphthyl moiety of (*S*)-configuration and asymmetric center moieties of (*S*)-, (*S*)-, (*R*)- and *racemic* configuration, linked with methylene spacers of 6, 12, 12 and 12, respectively. These chiral compounds were adopted as chiral dopants to induce chiral nematic liquid crystals (N*-LCs). The N*-LC including the double chiral dopant D-3, abbreviated as N*-LC with D-3 (system 2), showed an extraordinary increase in helical pitch (decrease in helical twisting power) in polarizing optical microscope (POM) when the temperature increased from 0 to 30 °C. This is due to a substantial cancellation in twisting power between the double chiral moieties having opposite screw directions, although both of them have the same (*S*)-configuration. Meanwhile, the N*-LC including the two types of chiral dopants D-1 and D-3, abbreviated as N*-LC with both D-1 and D-3 (system 3), exhibited a temperature-dependent helical inversion; It showed a notable increase in left-handed helical pitch when the temperature increased from 0 to 15 °C, and became a nematic phase giving no helicity in the temperature range of 16−19 °C, and then showed a right-handed N* phase giving a decrease in helical pitch when the temperature increased from 20 to 25 °C. The changes in helical sense and helical pitch in the N*-LC were found to be thermally reversible. The helical pitch-controllable N*-LC (system 2) enabled us to control the screw structure and the spiral morphology of the helical polyacetylene by changing only the polymerization temperature.

Introduction

Asymmetric polymerization in a chiral nematic liquid crystal (N*-LC), used as an asymmetric reaction field, has been attracting current interests, since it has been demonstrated to be promising for providing not only helical structure but also spiral morphology in π-conjugated polymers consisting of achiral repeating unit.[1] In fact, several types of helical conjugated homopolymers and copolymers have been successfully synthesized through chemical or electrochemical polymerization in N*-LC.[2] The N*-LC itself can be prepared by adding a small amount of chiral compound, as a chiral dopant or a chirality inducer, into a nematic liquid crystal (N-LC). It has been elucidated that the screw direction of the helical conjugated polymer is determined by helical sense of the N*-LC, and that the helical sense itself is controllable by selecting the chirality of the chiral dopant.[3] However, the spiral morphology and even the screw direction of the helical conjugated polymer cannot be changed nor modified after the polymerization, because the conjugated polymer, if without sufficiently long side chains,[4] is infusible and insoluble in organic solvent.[5] This means that two kinds of N*-LCs with opposite helical sense might be required for synthesizing helical conjugated polymers with opposite screw directions such as right- and left-handed screw structures. It is therefore desirable to create an advanced chiral dopant that can afford both helical sense and helical pitch-controllable N*-LC, so far as one tries to control the helical sense of the conjugated polymer by using only one kind of N*-LC.

Scheme 1. Design of Double Chirality-Based Chiral Compound

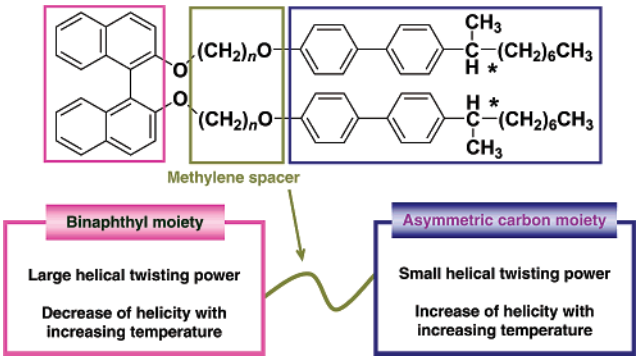

The thermally induced chiral inversion reported so far can be classified into two categories. One is to mix two kinds of N*-LCs, and another is to use one kind of N*-LC with peculiar temperature dependence in the helical sense. The former is furthermore classified into three approaches; (i) Two kinds of cholesterol derivatives with different helical twisting powers are added into N-LC.[6] (ii) Two kinds of cholesteric LCs with opposite helical sense[7] or (iii) even with the same helical sense[8] are mixed. On the other hand, the latter is also classified into two approaches. (iv) The N*-LC composed of double chiral center-containing compound with opposite helicity, different twisting power, and different temperature dependence is used.[9] (v) The N*-LC composed of single chiral center containing-

* Corresponding author. E-mail: akagi@star.polym.kyoto-u.ac.jp.
[†] Department of Polymer Chemistry, Kyoto University.
[‡] Institute of Materials Science, University of Tsukuba.
[§] Tsukuba Research Center for Interdisciplinary Materials Science (TIMS), University of Tsukuba.

10.1021/ma0703655 CCC: $37.00
Published on Web 06/16/2007

Scheme 2. Nematic LCs and Chiral Dopants, D-0−D-5

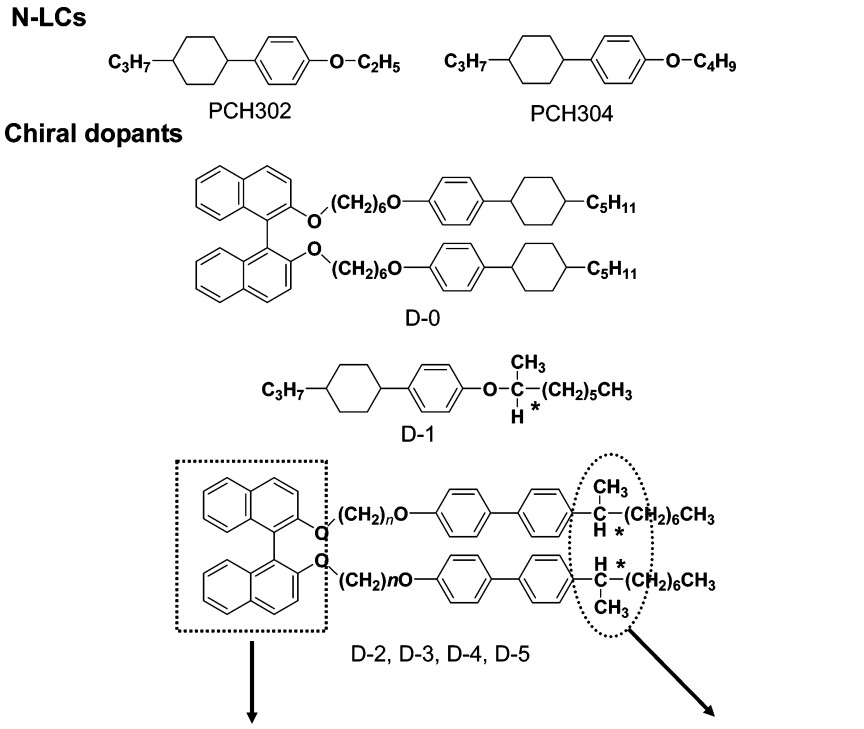

	Configuration of binaphthyl moiety	Methylene spacer, *n*	Configuration of asymmetric carbon moiety
D-2	*S*	6	*S*
D-3	*S*	12	*S*
D-4	*S*	12	*R*
D-5	*S*	12	*racemic*

compound is used.[10] The mechanism for the helical inversion using one kind of N*-LC still remains unclear.

The above-mentioned N*-LC or cholesteric LC, however, would not be available for the asymmetric reaction field, since the molecular species in the N*-LCs include several kinds of functional groups such as ester, carbonyl, ene, yne, and chlorine atom. Namely, these functional groups should be reactive to catalyst and/or monomers, which might cause to subreaction and even destruction of LC reaction field. From the viewpoint of asymmetric reaction field where the helicity of the N*-LC is replicated to the reaction product, it is essential to prepare the N*-LC composed of chemically stable and nonreactive LC molecules and chiral compounds. It is also desirable for practical use that the N*-LC is highly twisted, and that the temperature of the N*-LC is as close as to room temperature for the sake of safety, especially in the case of acetylene polymerization.

Here, we will focus on an axially chiral binaphthyl derivative as well as an asymmetric center-containing chiral compound. The former (binaphthyl derivative) is known to possess a large twisting power and thermal stability.[1,11] These properties are attributed to large steric repulsions between hydrogens at the 2 and 2′ positions and those at the 8 and 8′ ones in the binaphthyl rings.[12] It is suggested that the twisting power of the binaphthyl derivative might be almost independent of temperature, owing to its large thermal stability. Meanwhile, the latter (the asymmetric center-containing chiral compound), such as D-1, is found to exhibit an opposite temperature dependence in helical twisting power,[13,14] compared with the binaphthyl derivative. Hence it might be possible to prepare the helical inversion-controllable N*-LC by mixing both the binaphthyl compound and the asymmetric center-containing chiral one. Note that the chirality of the binaphthyl derivative can be changed by modifying the molecular structure even if the configuration remains unchanged.[1c,15] However, helical inversion utilizing temperature dependence has not been reported thus far.

In this work, to achieve a large temperature dependence in helical twisting power of the binaphthyl derivative, we designed the novel chiral compound where the binaphthyl moiety is linked with the asymmetric carbon moiety through flexible methylene chains in a molecule (Scheme 1). This is because the combination between the binaphthyl derivative with large temperature dependence and the asymmetric center-containing compound should allow us to control the helical pitch of the N*-LC and even to control the helical inversion, by virtue of different temperature dependence in helical twisting power between the two moieties. Here we present the novel N*-LCs which exhibit not only an extraordinarily large temperature dependence in the helical pitch but also a temperature-dependent helical inversion.

Experimental Section

Synthesis of Double Chirality Based Binaphthyl Derivatives. We synthesized an asymmetric center-containing phenylcyclohexyl (PCH) derivative, 4-(*trans*-4-*n*-propylcyclohexyl)-[(*S*)-2-methyl]-heptyloxybenzene (abbreviated as D-1). Subsequently, we synthesized novel double chiral based binaphthyl derivatives (abbreviated

Scheme 3. Synthetic Routes for the Asymmetric Center-Containing Axially Chiral Binaphthyl Derivatives

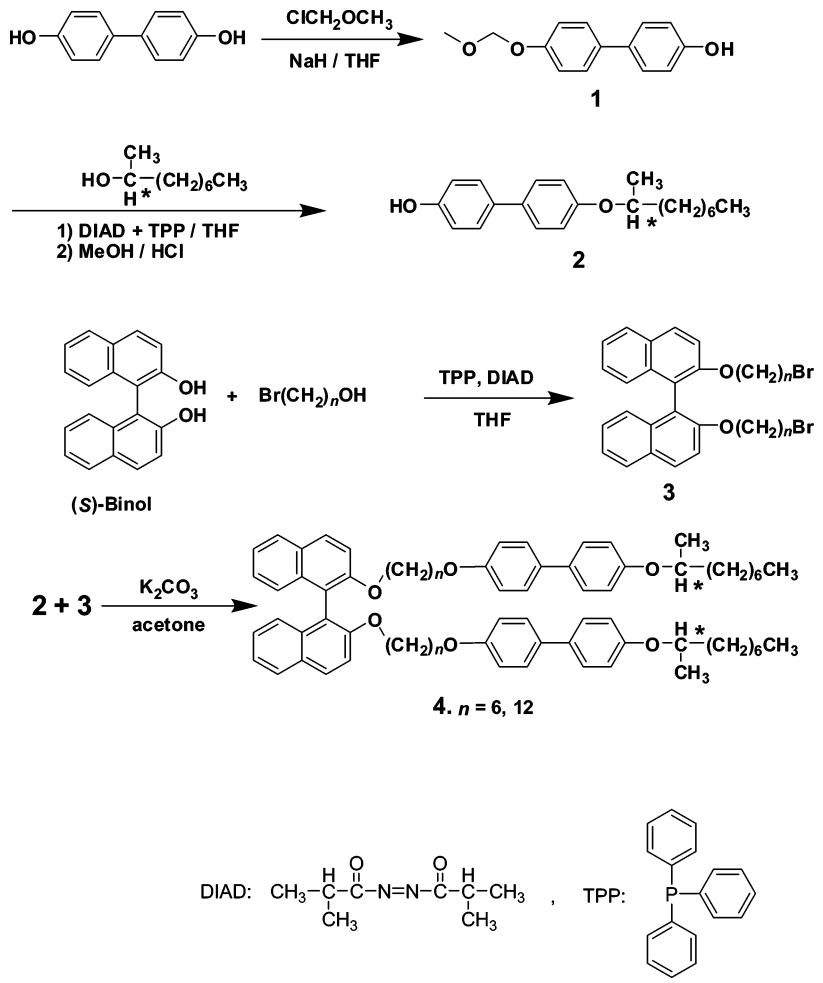

as D-2−D-5), where the biphenyl mesogenic moieties linked with chiral nonyl terminal group of (*S*)-, (*R*)- or *racemic* configuration are substituted at the 2,2′-positions of the binaphthyl ring via a hexyl or dodecyl methylene spacer, as shown in Scheme 2. For instance, D-3 is a (*S*)-1,1′-binaphthyl-2,2′-bis{*p*-[4-(*S*)-(2-methyl)-octyloxy]biphenyloxydodecyl} ether.

All experiments were performed under argon atmosphere. Tetrahydrofuran (THF), dichloromethane (CH_2Cl_2) and acetone were distilled prior to use. Williamson etherification and Mitsunobu etherification were used to obtain the chiral dopants. The chemical compounds, (*R*)- and (*S*)-2,2′-dihydroxy-1,1′-binaphthyl (optical purity: 0.99), were purchased from commercially available sources. The mesogenic compounds 4-(*trans*-4-*n*-propylcyclohexyl)phenol [PCH300] was purchased from Kanto Chemical Ltd. Here we abbreviated the name of liquid crystals as PCH302 and PCH304, which stand for 1-ethoxy-4-(*trans*-4-*n*-propylcyclohexyl)benzene and 1-butoxy-4-(*trans*-4-*n*-propylcyclohexyl)benzene, respectively.

Synthetic routes of the asymmetric center-containing axially chiral binaphthyl derivatives are shown in Scheme 3.

4-(Methoxymethyl ether)biphenyl-4′-ol (1). Biphenyl-4,4′-diol (2.0 g, 10.7 mmol) was dissolved in anhydrous THF (20 mL) and stirred at 0 °C. NaH (0.14 g, 5.6 mmol) was added to the solution at 0 °C. The mixture was stirred for 0.5 h at room temperature. Chloromethyl methyl ether (0.4 mL, 5.6 mmol) was added dropwise to the mixture. After 1 h, the reaction mixture was cooled to 0 °C and quenched with H_2O and extracted with $CHCl_3$. The organic layer was dried over with Na_2SO_4. The solvent was removed in vacuo after filtration. The organic layer was subjected to chromatography on silica using CH_2Cl_2 as an eluent to give a white powder, **1** (1.2 g, 48%). Anal. Calcd for $C_{14}H_{14}O_3$: C, 73.03; H, 6.13. Found: C, 72.85; H, 6.33. ^{1}H NMR (400 MHz, $CDCl_3$, δ from TMS, ppm): δ = 3.50 (s, 3H, −OCH_3), 5.21 (s, 2H, Ar−O−CH_2−O−), 6.86−6.87 (d, 2H, J = 5.6, phenyl), 7.07−7.09 (d, 2H, J = 7.2, phenyl), 7.40−7.47 (m, 4H, phenyl). ^{13}C NMR (400 MHz, $CDCl_3$, δ from TMS, ppm): 56.04, 94.45, 115.48, 115.53, 116.38, 116.47, 127.67, 133.45, 138.1, 154.64, 156.13. HRMS (FAB, *m/z*): calcd, 230.0943; found, 230.0947.

4-{(*S*)-2-Nonanyloxy}biphenyl-4′-ol (2). A solution of **1** (0.45 g, 2.0 mmol), (*R*)-, (*S*)-, or *racemic*-2-nonanol (0.34 g, 2.4 mmol), and triphenylphosphine (0.62 g, 2.4 mmol) in anhydrous THF (10 mL) was added dropwise to azodicarboxylic acid diisopropyl ester (1.2 mL, 2.4 mmol) at 0 °C. It was stirred at room temperature overnight and extracted with $CHCl_3$. The organic layer was washed twice with water and dried over with Na_2SO_4. The solvent was removed in vacuo after filtration. The organic layer was subjected to chromatography on silica using CH_2Cl_2/*n*-hexane = 3/1 as an eluent to give a white powder, 4-(methoxymethyl ether)-4′-{(*S*)-2-nonanyloxy}biphenyl (0.5 g, 72%). 4-(methoxymethyl ether)-4′-{(*S*)-2-nonanyloxy}biphenyl (0.5 g, 1.4 mmol) was dissolved in methanol (50 mL) and small amount of HCl was added to the solution. The reaction mixture was refluxed for 1 h and extracted with $CHCl_3$. The organic layer was washed twice with water and dried over with Na_2SO_4. The solvent was removed in vacuo after filtration. The organic layer was subjected to chromatography on silica using CH_2Cl_2 as an eluent to give a white powder, **2** (0.35 g, 80%). Anal. Calcd for $C_{21}H_{28}O$: C, 80.73; H, 9.03. Found: C, 80.72; H, 9.59. ^{1}H NMR (400 MHz, $CDCl_3$, δ from TMS, ppm) : 0.86−0.89 (t, 3H, J = 6.7, CH_3), 1.27−1.78 (m, 15H, CH_2), 4.35−4.40 (q, 1H, J = 5.9, Ar−O−CH−CH_3), 5.0 (s, 1H, -*OH*), 6.85−6.95 (m, 4H, phenyl), 7.24−7.45 (m, 4H, phenyl). ^{13}C NMR (400 MHz, $CDCl_3$, δ from TMS, ppm): 14.17, 19.86, 22.72, 25.66, 29.32, 31.85, 36.54, 74.15, 115.51, 116.06, 127.63, 127.83, 133.08, 133.67, 154.38, 157.16. HRMS (FAB, *m/z*): calcd, 312.2089; found, 312.2081.

(*S*)-2,2′-Bis(12-bromododecyloxy)-1,1′-binaphthyl (3, *n* = 12). The solution of (*S*)-1,1′-binaphthyl-2,2′-diol (2 g, 7 mmol), 12-bromodedecan-1-ol (5.56 g, 21 mmol), and triphenylphosphine (4.6 g, 17.5 mmol) in anhydrous THF (15 mL) was added dropwise to azodicarboxylic acid diisopropylester (10 mL, 21 mmol) at 0 °C. It was stirred at room temperature overnight and extracted with $CHCl_3$. The organic layer was washed twice with water and dried over with Na_2SO_4. The solvent was removed in vacuo after filtration. The organic layer was subjected to chromatography on silica using CH_2Cl_2/*n*-hexane = 3/1 as an eluent to give a colorless oil, **3**, *n* = 12 (4 g, 74%). Anal. Calcd for $C_{44}H_{60}Br_2O_2$: C, 67.69; H, 7.75. Found: C, 67.87; H, 7.73. ^{1}H NMR (400 MHz, $CDCl_3$, δ from TMS, ppm): 0.88−1.43 (m, 36H, CH_2), 1.83−1.87 (m, 4H, $-CH_2-CH_2O$, $-CH_2-CH_2Br$), 3.38−3.42 (t, 4H, *J* = 5.4, CH_2-Br), 3.85−3.95 (m, 4H, Ar−OCH_2), 7.13−7.91 (m, 12H, Ar-*H*). ^{13}C NMR (400 MHz, $CDCl_3$, δ from TMS, ppm): 25.62, 28.22, 28.83, 29.15, 29.41, 29.44, 29.56, 32.87, 34.11, 69.72, 115.76, 120.60, 123.26, 125.38, 125.88, 127.64, 128.88, 129.11, 134.09, 154.36. HRMS (FAB, *m/z*): calcd, 780.2940; found, 780.2965.

(*S*)-2,2′-Bis{12-[4-(*S*)-(2-nonanyloxy)biphenyl-4-yloxy]dodecyloxy}-1,1′-binaphthyl (D-3). Compound **2** (0.59 g, 1.88 mmol) and compound **3** (*n* = 12, 0.66 g, 0.85 mmol) and K_2CO_3 (0.26 g, 1.88 mmol) were dissolved in acetone (20 mL). The mixture was stirred for 12 h at 60 °C, and then it was extracted with H_2O and $CHCl_3$. The organic layer was dried over with Na_2SO_4. The solvent was removed in vacuo after filtration. The organic layer was subjected to chromatography on silica using CH_2Cl_2/*n*-hexane = 1/1 as an eluent to give a colorless oil, **4** (D-3, 0.98 g, 93%). Anal. Calcd for $C_{86}H_{114}O_6$: C, 83.04; H, 9.24. Found: C, 83.0; H, 9.01. ^{1}H NMR (400 MHz, $CDCl_3$, δ from TMS, ppm) : 0.86−1.59 (m, 70H, CH_2, CH_3), 1.70−1.83 (m, 6H, −O−CH−CH_3), 3.85−3.98 (m, 8H, Ar−O−CH_2−), 4.34−4.38 (m, 2H, Ar−OCH−), 6.90−6.96 (m, 8H, phenyl), 7.13−7.20 (m, 4H, Ar−*H*), 7.26−7.30 (m, 2H, phenyl), 7.37−7.49 (m, 10H, phenyl), 7.81−7.91 (m, 4H, Ar−*H*). ^{13}C NMR (400 MHz, $CDCl_3$, δ from TMS, ppm): 14.17, 19.89, 22.72, 25.66, 26.16, 29.19, 29.33, 29.40, 29.45, 29.50, 29.64, 31.64, 31.87, 36.59, 68.07, 69.77, 73.99, 114.66, 115.80, 116.01, 120.66, 123.28, 125.42, 125.90, 126.60, 127.60, 128.60, 129.17, 133.16, 133.26, 134.14, 154.42, 157.20, 158.10. HRMS (FAB, *m/z*): calcd, 1242.8615; found, 1242.8612.

(*S*)-2,2′-Bis{6-[4-(*S*)-(2-nonanyloxy)biphenyl-4-yloxy]hexyloxy}-1,1′-binaphthyl (D-2). Anal. Calcd for $C_{74}H_{90}O_6$: C, 82.64; H, 8.43. Found: C, 82.42; H, 8.34. ^{1}H NMR (400 MHz, $CDCl_3$, δ from TMS, ppm): 0.86−1.56 (m, 52H, CH_2, CH_3), 3.71−3.97 (m, 8H, Ar−O−CH_2−), 4.33−4.35 (m, 2H, Ar−OCH), 6.86−6.92 (m, 8H, phenyl), 7.17−7.40 (m, 16H, Ar−*H*), 7.80−7.88 (m, 4H, Ar−*H*). ^{13}C NMR (400 MHz, $CDCl_3$, δ from TMS, ppm): 14.17, 19.83, 22.69, 25.44, 25.63, 29.05, 29.30, 29.62, 31.83, 36.53, 67.70, 69.58, 73.89, 114.58, 115.45, 115.76, 115.95, 120.62, 123.35, 125.36, 125.94, 127.45, 127.50, 127.53, 127.68, 128.97, 129.14, 133.05, 133.13, 134.05, 154.30, 157.11, 157.96. MS (MALDI−TOF, *m/z*): calcd, 1074.67; found, 1074.14.

(*S*)-2,2′-Bis{12-[4-(*R*)-(2-nonanyloxy)biphenyl-4-yloxy]dodecyloxy}-1,1′-binaphthyl (D-4). Anal. Calcd for $C_{86}H_{114}O_6$: C, 83.04; H, 9.24. Found: C, 82.80; H, 9.25. ^{1}H NMR (400 MHz, $CDCl_3$, δ from TMS, ppm) : 0.86−1.81 (m, 76H, CH_2, CH_3), 3.93−3.98 (m, 8H, Ar−O−CH_2−), 4.34−4.38 (m, 2H, Ar−OCH), 6.90−6.94 (m, 8H, phenyl), 7.15−7.28 (m, 6H, Ar−*H*), 7.37−7.46 (m, 10H, phenyl), 7.82−7.91 (m, 4H, Ar−*H*). ^{13}C NMR (400 MHz, $CDCl_3$, δ from TMS, ppm): 14.18, 19.87, 22.72, 25.66, 25.67, 26.16, 29.19, 29.33, 29.39, 29.43, 29.50, 29.52, 29.65, 31.87, 36.58, 68.04, 69.74, 73.96, 114.62, 115.78, 115.98, 120.62, 123.27, 125.41, 125.90, 127.54, 127.59, 127.66, 128.91, 129.14, 133.13, 133.23, 134.11, 154.39, 157.16, 158.06. HRMS (FAB, *m/z*): calcd, 1242.8615; found, 1242.8586.

(*S*)-2,2′-Bis{12-[4-(*rac*)-(2-nonanyloxy)biphenyl-4-yloxy]dodecyloxy}-1,1′-binaphthyl (D-5). Anal. Calcd for $C_{86}H_{114}O_6$: C, 83.04; H, 9.24. Found: C, 82.86; H, 9.13. ^{1}H NMR (400 MHz, $CDCl_3$, δ from TMS, ppm): 0.87−1.81 (m, 76H, CH_2, CH_3), 3.89−4.00 (m, 10H, Ar−O−CH_2-), 6.92−6.94 (m, 8H, phenyl), 7.15−7.46 (m, 16H, Ar−*H*), 7.82−7.92 (m, 4H, Ar−*H*). ^{13}C NMR (400 MHz, $CDCl_3$, δ from TMS, ppm): 14.20, 22.74, 24.85, 25.66, 26.13, 26.15, 29.19, 29.33, 29.37, 29.39, 29.43, 29.48, 29.49, 29.52, 29.61, 29.64, 31.93, 68.07, 69.75, 114.64, 115.79, 120.62, 123.27, 125.41, 125.90, 127.55, 127.66, 128.91, 129.14, 133.19, 133.22, 134.11, 154.40, 158.08. HRMS (FAB, *m/z*): calcd, 1242.8615; found, 1242.8610.

Proton (^{1}H) and carbon (^{13}C) nuclear magnetic resonance (NMR) spectra were measured in $CDCl_3$ using a JEOL 400 MHz NMR spectrometer. Chemical shifts are expressed in parts per million downfield from tetramethylsilane as an internal standard. The chemical properties of the compounds synthesized are given in the last section. Elemental analyses were performed at the Analytical Center of University of Tsukuba and Microanalytical Center of Kyoto University. High-resolution mass spectra (HRMS) were measured at the Technical Center of Department of Synthetic Chemistry and Biological Chemistry of Kyoto University.

Preparation of N*-LC. The N*-LCs were prepared by adding a small amount of chiral dopant into an equimolar mixture of two kinds of N-LCs of PCH302 and PCH304. It should be noted that although each compound (PCH302 or PCH304) shows N-LC phase, the LC temperature region is very narrow, i.e., less than 1−2 deg. This is not suitable for acetylene polymerization in a nematic or chiral nematic LC reaction field, because the exothermal heat evoking during the acetylene polymerization would increase the temperature inside the polymerization vessel and easily destroy the LC phase. Hence, we prepared the LC mixture by using the equimolar two LCs. In the LC mixture, the nematic−isotropic temperature, T_{N-I}, and the crystalline-nematic temperature, T_{C-N}, were raised and lowered, respectively. Actually, the mixture exhibited the N-LC phase in the temperature region from 20 to 35 °C. Three kinds of N*-LCs were prepared by adding the chiral dopants into the equimolar mixture of PCH nematic LC (Table 1). Because of the effect of supercooling, the N*-LC phase consisting of the LC mixture and the chiral dopants were maintained in the temperature range from 0 to 30 °C. This sufficiently wide temperature region allowed us to examine the feasibility for the helical inversion in the present N*-LC system.

Measurement of Helical Pitch and Helical Sense of N*-LC. Polarized optical microscope (POM) observation was carried out under crossed nicols by using a Nikon ECLIPSE E 400 POL microscope equipped with a Nikon COOLPIX 950 digital camera.

The helical pitch of the N*-LC was measured by Cano wedge method using the POM.[16] When the N*-LC was inserted into a wedge-type cell with gradient thickness, the discontinuity lines named Cano lines appeared on the surface of the cell under the crossed nicols. The helical pitch (*p*) was evaluated by measuring the distance between the Cano lines. On the other hand, the helical sense of the N*-LCs were examined through the miscibility test.[1c,17] The mixing area between the N*-LC and a standard LC was observed under the POM. When the screw direction of the N*-LC is the same as that of the standard LC, the mixing area should be continuous. However, there should appear a discontinuous boundary (a *Schlieren* texture characteristic of N-LC) between the N*-LC and the standard LC, when they have opposite directions each other. The cholesteryl oleyl carbonate, known to be left-handed, was used as the standard LC for the miscibility test.

Polymerization of Acetylene. Acetylene gas of six-nine grade and triethylaluminum, $AlEt_3$, were used without further purification. Tetra-*n*-butoxytitanium, Ti(O-*n*-Bu)$_4$, was distilled under argon gas prior to use. Equimolar mixture of liquid crystals was used as polymerization solvents without further purification, except degassing prior to use. Concentration of the catalyst was 0.05 M of Ti(O-*n*-Bu)$_4$, and the ratio of $AlEt_3$ to Ti(O-*n*-Bu)$_4$ was 4.0. The catalyst solution was aged for 30 min at room temperature. Apparatus and procedure employed were the same as those of the previous work except for polymerization temperature.[1] Polymerization temperature was controlled by covering Schlenk flask with circulating coolant through an outer flask which envelops the Schlenk flask. Temperature was monitored through a thermometer located under a flat-bottom container for the catalyst solution. Initial acetylene pressure was about 30 Torr. The polymerization was

Table 1. Mixing Mole Ratios between the Parent N-LCs and the Chiral Dopants in N*-LCs, Systems 1, 2, and 3

N-LCs	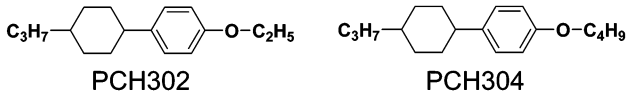 PCH302 PCH304
Chiral dopants	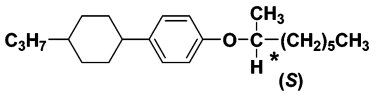 D-1 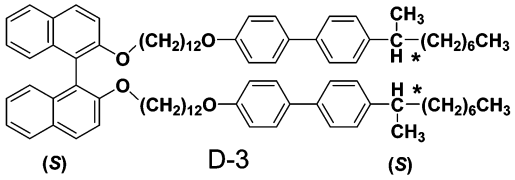 (S) D-3 (S)
System 1	PCH302 : PCH304 : D-1 = 100 : 100 : 7 (in mole ratio)
System 2	PCH302 : PCH304 : D-3 = 100 : 100 : 2 (in mole ratio)
System 3	PCH302 : PCH304 : D-1 : D-3 = 100 : 100 : 7 : 2 (in mole ratio)

stopped when the pressure was decreased by 5 Torr. After the polymerization, polyacetylene film was carefully stripped off from the container and washed with toluene several times under Argon gas, and then dried on a Teflon sheet in vacuo for 2 h. The dried film was kept under argon in a freezer at −20 °C before measurements.

Observation of Scanning Electron Microscope (SEM). Morphologies of helical polyacetylene films were observed using a SEM with type of DS-130 (TOPCON). Before measurements of SEM, the polyacetylene films were coated with Pt−Pd alloy using an ion coater with type of IB-5 (EIKO). The coating thickness was evaluated to be ca. 10 nm. The SEM operation was performed under an acceleration voltage of 10 kV. Note that the helical pitch and the spiral morphology of the helical polyacetylene remained unchanged during the Pt−Pd alloy coating and the SEM observation, owing to the infusibility of helical polyacetylene.

Results and Discussion

Temperature Dependence of N*-LCs. Figure 1 shows a temperature dependence of the helical pitch (p) and helical twisting power (β) of the N*-LC, which was induced by adding the axially chiral binaphthyl compound, PCH506-Binol of (R)-configuration (abbreviated as D-0), into the equimolar mixture of PCH nematic LC. The PCH506-Binol was synthesized according to the previously reported procedure.[1,11] It is clear that the binaphthyl derivative has a large twisting power and a small temperature dependence. These properties are attributed to large steric repulsions between hydrogens at the 8- and 8′-positions in the binaphthyl rings.[12]

Next, the N*-LC was prepared by adding the asymmetric center containing chiral dopant (D-1) into the equimolar mixture of PCH nematic LC (system 1). The N*-LC induced by the D-1 of (S)-configuration was found to have a right-handed screw structure, and it showed a notable temperature dependence in helical pitch or in helical twisting power.[9] Namely, the helical pitch (the helical twisting power) decreases (increases) with increasing temperature, as also shown in Figure 1. This unusual

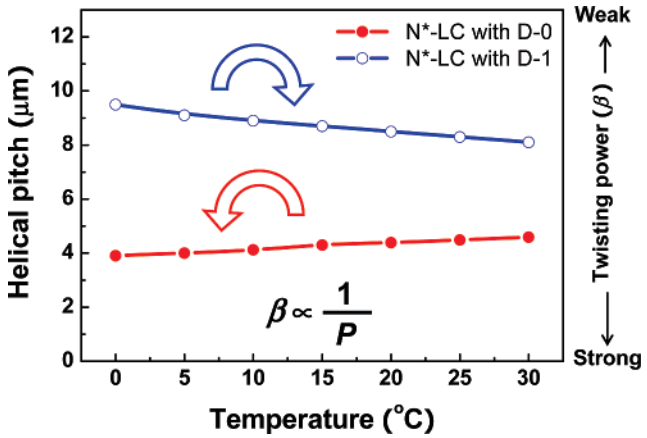

Figure 1. Temperature dependence of the helical pitch (p) and helical twisting power (β) of the N*-LC induced by the axially chiral binaphthyl derivative, PCH-506-Binol of (R)-configuration (D-0) (PCH302:PCH304:D-0 = 100:100:2 in mole ratio) or the asymmetric center-containing chiral compound of (S)-configuration, (D-1) (system 1). The helical pitch was determined by Cano's wedge cell method. The twisting power (β) was calculated as $\beta = (pcr)^{-1}$, where c is the mole fraction of the chiral dopant and r is the enantiometric purity of the chiral dopant. Here, r is assumed to be 1.

temperature dependence is probably due to the fact that the miscibility of the chiral dopant (D-1) in the host nematic LC increases with increasing temperature. Better miscibility enables the chiral dopant to affect more effectively its helicity to the environmental N-LC molecules, which leads to an increases in twisting power (decrease in helical pitch). It should be noted that the asymmetric center containing chiral compound, such as D-1, has an opposite temperature dependence in helical twisting power (β), compared with that of the binaphthyl derivative, although the absolute value of β in the former is considerably smaller than that of the latter. Hence, if two kinds of chiral molecules with opposite temperature dependence and different twisting powers are linked by a certain flexible unit,

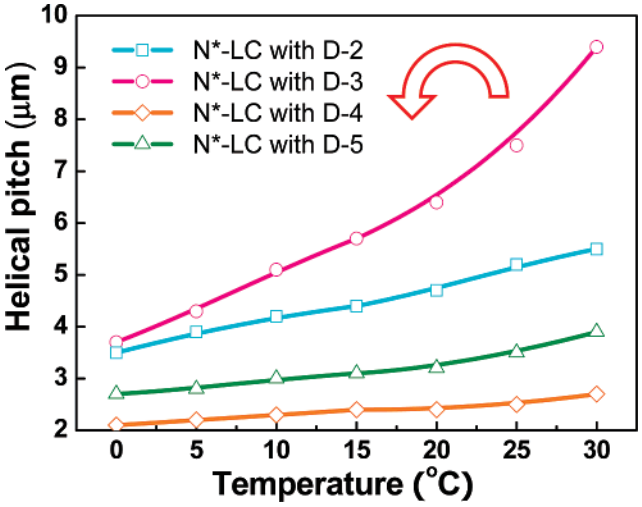

Figure 2. Temperature dependence of the helical pitch of the N*-LCs induced by the chiral dopant of D-2−D-5 (PCH302:PCH304:chiral dopant = 100:100:2 in mole ratio).

the resultant compound having double chirality might exhibit peculiar temperature dependence (Scheme 1).

Then, we designed and synthesized the novel double chiral compounds, D-2−D-5, where the axially chiral binaphthyl moiety is linked with the asymmetric carbon moiety through flexible methylene chains in a molecule (Scheme 2). Four kinds of N*-LCs were prepared by adding the chiral dopants of double chirality based binaphthyl derivatives (D-2−D-5) into the equimolar mixture of PCH nematic LC (PCH302:PCH304:D-2−D-5 = 100:100:2 in mole ratio). It has been clarified that the axially chiral binaphthyl derivatives of (*S*)-configuration and the asymmetric-center moiety containing chiral dopants of (*S*)-configuration induce left- and right-handed N*-LCs, respectively, when each of them is added into the N-LC.[1,9] Interestingly, the dopants D-2−D-5, bearing both the binaphthyl moiety and the asymmetric-center containing moiety, induced left-handed N*-LC. This result implies that the helicity of the binaphthyl moiety is much larger than that of the asymmetric center-containing moiety. For instance, the chiral dopant of D-3 (system 2) induces a left-handed screw structure, even after a partial cancellation of helicity between the two moieties. The temperature dependence in the helical pitch of the N*-LCs was investigated as shown in Figure 2. In the Cano wedge type cell, the helical pitch of the N*-LC with D-3 notably changed from 3.7 to 9.4 μm with increasing temperature from 0 to 30 °C, while the left-handed screw structure remained unchanged through the whole range of temperature.

We also examined the effect of the spacer length (*n*) which links the binaphthyl moiety and the asymmetric center moiety. The methylene spacer of the chiral dopants D-2 and D-3 are 6 and 12, respectively. The longer spacer allows both the chiral moieties to be less restricted in molecular motion, enabling more free arrangement toward the environmental LCs. Taking into account that the binaphthyl and asymmetric center moieties with the same configurations have opposite helical twisting directions, the helical cancellation in D-3 with the spacer length of 12 should be larger than that in D-2 with the spacer length of 6. Namely, both chiral moieties, especially the asymmetric-center moiety, in D-3 would be more effectively enhanced in molecular motion with increasing temperature. This should cause to a larger helical cancellation and hence a more drastic increase in helical pitch of the N*-LC, than the case of D-2. Meanwhile, since the binaphthyl moiety of (*S*)-configuration and the asymmetric moiety of (*R*)-configuration induce the same twisting direction (left-handed) in N*-LC, no cancellation occurs in the case of D-4. Thus, the temperature dependence of the N*-LC with D-4 is the smallest one.

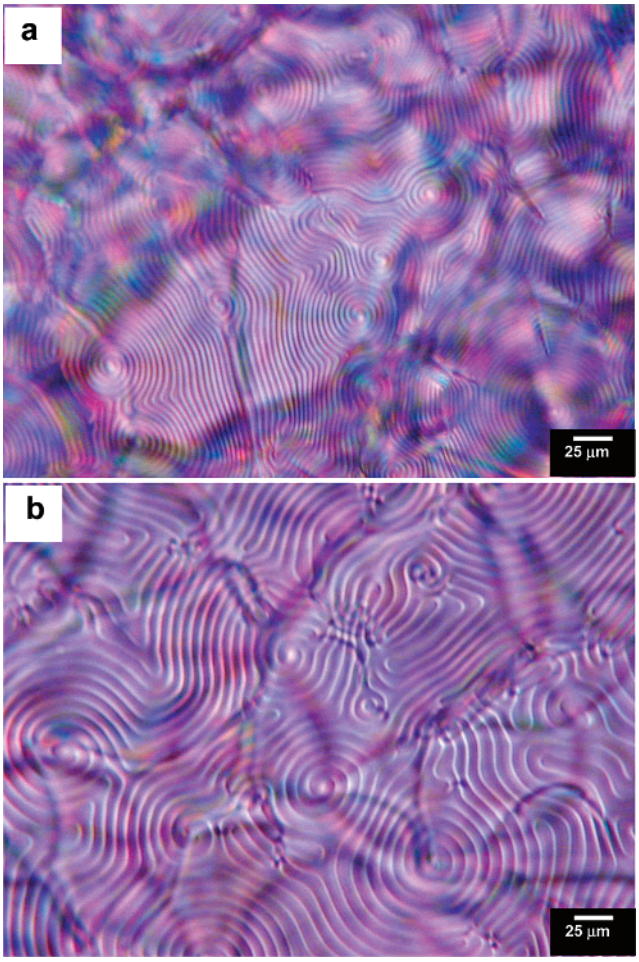

Figure 3. Finger print textures with striae observed in POM measurement for the N*-LC with D-3 (system 2) at 5 (a) and at 30 °C (b).

Figure 3 shows polarizing optical micrographs (POMs) of the N*-LC induced by D-3 (system 2) at 5 and 30 °C in the cooling processes. The interdistance of striae, corresponding to a half-helical pitch of the N*-LC, was 2.1 μm at 5 °C. It increased to be 4.6 μm with increasing temperature up to 30 °C. These changes in helical pitch were confirmed to be thermally reversible, owing to the enantiotropic nature of the present N*-LC.

Figure 4 schematically represents the temperature dependence of the N*-LC induced by D-3 (system 2). The helicity of the binaphthyl moiety and that of the asymmetric moiety decreased and increased with increasing of temperature, respectively. Although the sum of the helicity becomes smaller due to a part cancellation between the two moieties of opposite helical sense at each temperature, it exhibits an unprecedented temperature dependence in the helical twisting power of the N*-LC including D-3.

Figure 5 shows changes of the ratio in the helical pitch (P/P_0) as a function of temperature, where P and P_0 are the helical pitches of the N*-LC at arbitrary temperature and at 0 °C, respectively. It has been reported that the value (P/P_0) of N*-LC induced by the binaphthyl derivative, such as D-0, bearing two LC moieties at 2 and 2′ positions of the binaphthyl rings, is 1.2 (see Figure 1). Meanwhile, the value of the N*-LC

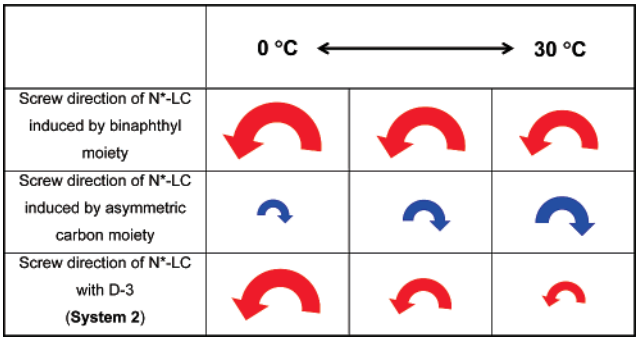

Figure 4. Schematic representation of temperature-dependent helical sense for the N*-LC with D-3. The arrows represent the screw directions of the N*-LCs, and the sizes of the arrows represent the degree of the twisting powers of the chiral dopants.

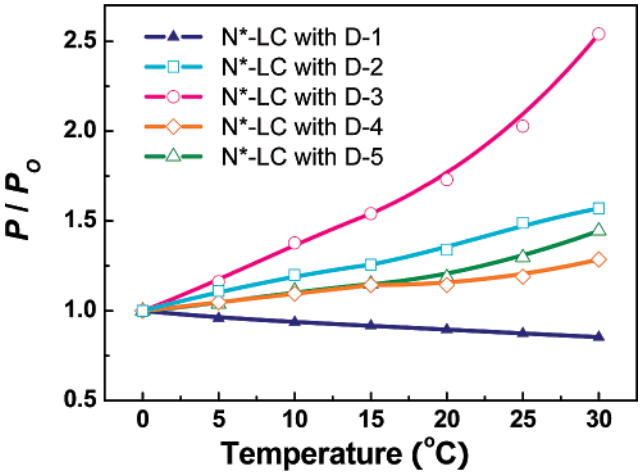

Figure 5. Changes of the ratio in helical pitch, defined as P/P_0, as a function of temperature. P and P_0 are the helical pitches of the N*-LCs at arbitrary temperature and 0 °C, respectively. The N*-LCs were prepared by D-1 (system 1) or D-2−D-5 (PCH302:PCH304:chiral dopant = 100:100:2 in mole ratio).

induced by D-3 (system 2) was more than 2.5, indicating a large temperature dependence. The N*-LCs with D-2−D-5 showed positive temperature dependence in change of helical pitch, and the temperature dependence of the N*-LC with D-3 (system 2) was much larger than those of others. Note that the N*-LC with D-1 (system 1) only showed negative temperature dependence. Thus, it is expected that the chiral dopants of D-1 and D-3 might be useful to realize the helical inversion of N*-LC, when they are added simultaneously as double chiral dopants with an appropriate mole ratio in N-LC.

Synthesis of Helical Polyacetylene in Helical Pitch-Controllable N*-LC. The helical pitch-controllable N*-LC (system 2) was actually used as a reaction field for acetylene polymerization. The acetylene polymerizations were carried out at 0, 10, and 20 °C, where the half helical pitches of N*-LC were 1.9, 2.6, and 3.4 μm, respectively. Figure 6 shows a scanning electron microscope (SEM) photograph of helical polyacetylene film synthesized at 10 °C. A typical spiral morphology of multidomain structure can be observed. It is worthy noting that the spiral morphology is composed of bundles of fibrils and that the fibril itself is a bundle of helical polyacetylene chains. Such hierarchical spiral structures are characteristics of the helical polyacetylene synthesized in chiral nematic liquid crystal.[1] The SEM photographs of helical polyacetylenes synthesized at 0 and 20 °C are given in the Supporting Information. Figure 7 shows POMs of the N*-LCs (system 2) and SEM photographs of the helical polyacetylene

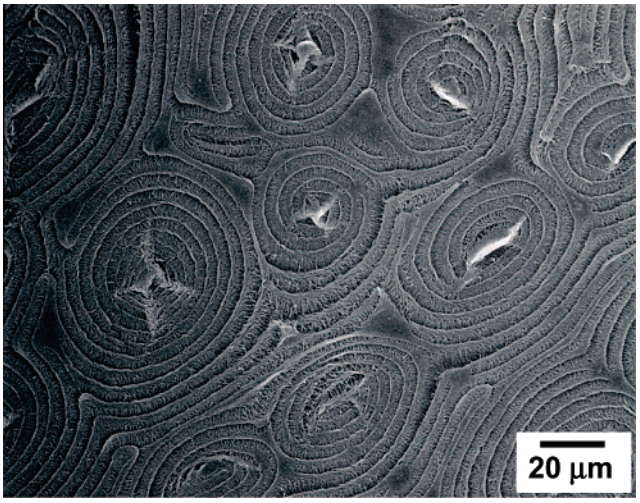

Figure 6. SEM photograph of multidomain spiral structure in helical polyacetylene synthesized under N*-LC with D-3 (system 2) at 10 °C.

films synthesized at 0, 10, and 20 °C. The polyacetylene films exhibit spiral fibril morphologies which are quite similar to those of the N*-LCs. It was confirmed that the polyacetylene fibrils screwed clockwise to form helical bundles of fibrils, and that the bundles gave rise to the spiral morphology with one-handed screw direction.

It has been elucidated hitherto that the interdistance (a) between the fibril bundles of the helical polyacetylene is correlated with the half of the helical pitch (p) of the N*-LC, i.e., $a = p/2$.[1] It means that the interdistance of the fibril bundles can be an index to evaluate not only the degree of the twisting of the helical polyacetylene but also that of the N*-LC used as a solvent. The interdistances of the helical polyacetylenes synthesized at 0, 10, and 20 °C were 2.1, 2.9, and 3.6 μm, respectively. They are very close to halves of the helical pitches (1.9, 2.6, and 3.4 μm) of the N*-LC observed at 0, 10, and 20 °C, respectively (see, Figure 7). This result indicates that both the screw structure and the spiral morphology of the helical polyacetylene are well controlled by changing only the polymerization temperature, when the present helical pitch-controllable N*-LC is used as the asymmetric reaction field. Note that the slightly larger values of the interdistances for the helical polyacetylenes, in comparison with the halves of the helical pithces of the N*-LCs, are due to the exothermic heat evolving during the acetylene polymerization. Namely, the exothermic heat would rise the polymerization temperature to increase the helical pitch of the N*-LC used as the polymerization solvent.

Helical Inversion Controllable N*-LC. Figure 8 shows changes in the helical pitch of the right-handed N*-LC induced by D-1 (system 1) and the left-handed N*-LC induced by D-3 (system 2), as a function of temperature. The helical pitches of system 1 and system 2 respectively decrease and increase with increasing temperature, and they are crossed at 26 °C. This suggests that the helical inversion might occur in the N*-LC when both D-1 and D-3 are mixed as two kinds of chiral dopants. Then, we prepared the N*-LC (system 3) by adding these chiral dopants with appropriate ratio into N-LC. Figure 9 shows changes in helical pitch of system 3 as a function of temperature. The polarized optical micrographs of the system 3 are shown in Figure 10. The helical pitch of 4.7 μm at 0 °C increased and became undetectable near 16 °C, as temperature increased. On further heating, the finger print texture reappeared near 20 °C, and the helical pitch decreased to 15 μm at 25 °C.

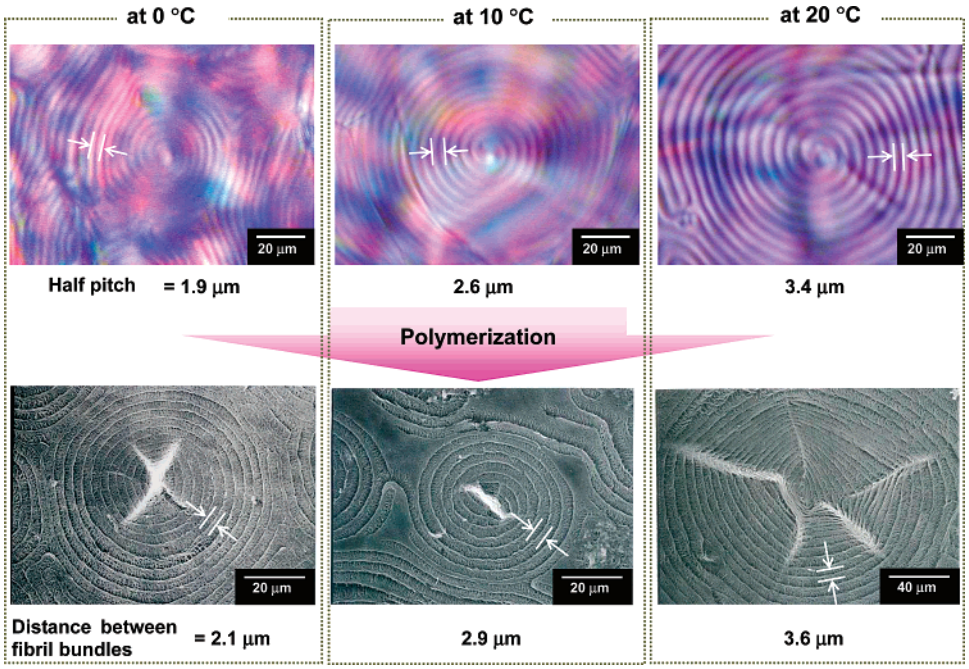

Figure 7. POM textures of N*-LC with D-3 (system 2) at 0 (left), 10 (middle), and 20 °C (right), and SEM photographs of helical polyacetylene synthesized in N*-LC with D-3 at 0 (left), 10 (middle), and 20 °C (right).

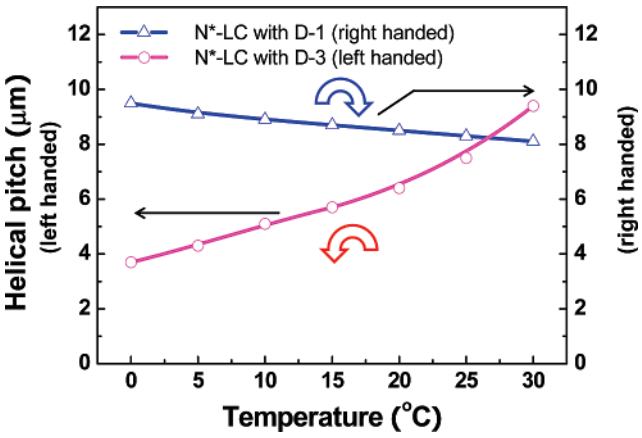

Figure 8. Temperature dependence of the helical pitches of the N*-LCs with D-1 (system 1) and D-3 (system 2).

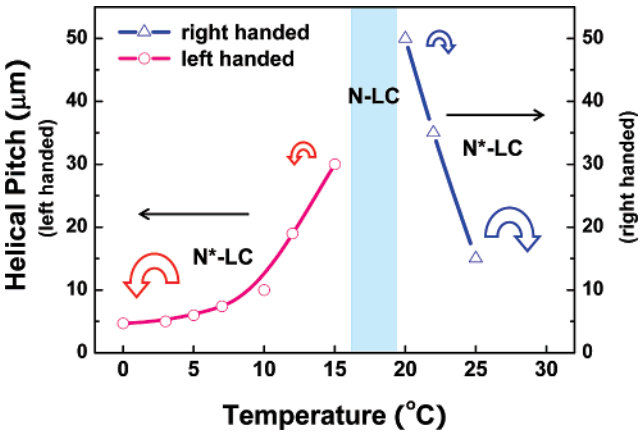

Figure 9. Temperature dependence of the helical pitch of the N*-LC with both D-1 and D-3 (system 3).

Above 25 °C, the N*-LC phase changed into isotropic one. The N*-LC showed not only a fast response to temperature change but also a good reversibility in the temperature region from 0 to 25 °C. As shown in Figure 8, the curves for the helical pitches of system 1 and system 2 are crossed at 26 °C, but the N-LC phase appeared from 16 to 19 °C. This temperature region (from 16 to 19 °C) can be regarded as the compensation point between the two kinds of the chiral dopants with opposite helical sense (D-1 and D-3) when dissolved in one N-LC.

Subsequently, the helical sense of the N*-LC including both D-1 and D-3 (system 3) was examined through the miscibility test. The POM photographs of the mixing area between the N*-LC and the cholesteryl oleyl carbonate as a standard LC was also shown in Figure 10. The mixing area was continuous from 0 to 15 °C, indicating that the screw direction of the N*-LC in this temperature region is the same as that of the standard LC. However, from 16 to 19 °C, there appeared a discontinuous boundary, showing a *Schlieren* texture characteristic of nematic LC, between the N*-LC and the standard LC. The finger print texture reappeared in the range from 20 to 25 °C, and the screw direction was found to be opposite to that of the standard LC, i.e., right-handed. This means that the screw directions of the N*-LC below and above the compensation point (from 16 to 19 °C) are opposite each other, indicating an occurrence of helical inversion.

The helical inversion in the N*-LC including both D-1 and D-3 (system 3) is schematically described in Figure 11. At low temperature, the twisting power of D-3 is larger than that of D-1, thus the sum of the twisting powers with opposite directions (D-1 and D-3) gives the same screwed direction (left-handed) as that of the N*-LC with D-3. The twisting power of D-1 increases with increasing temperature, and then becomes equal to that of D-3 at 16 °C. At this point (compensation point), the twisting powers with opposite directions of D-1 and D-3 cancel out each other, giving a nematic phase. With increasing temperature, the twisting power of D-1 further increases and becomes larger than that of D-3. This gives rise to right-handed screw direction at high temperature, leading to a helical inversion in the N*-LC. Acetylene polymerization using the helical inversion-controllable N*-LC is now underway and the results are to be reported somewhere in the near future.

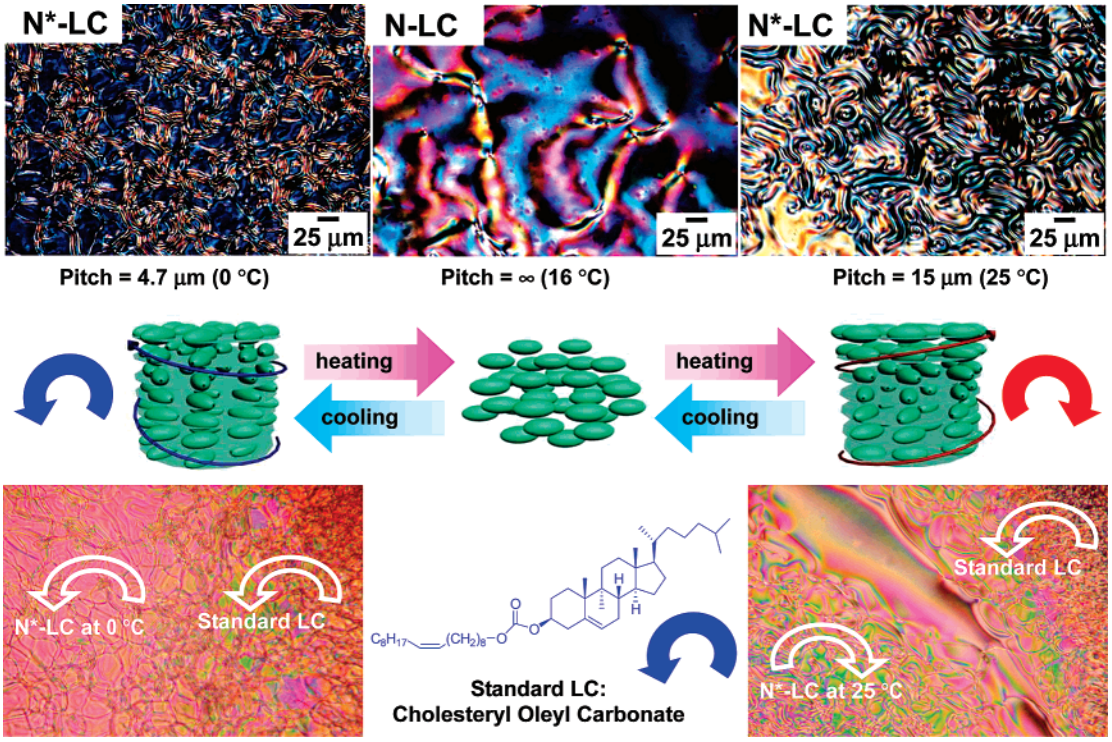

Figure 10. POM textures of N*-LC with both D-1 and D-3 by changing temperature (upper), and the miscibility tests between the N*-LC and standard cholesteric LC (lower). The helical sense of the N*-LC (system 3) was examined through the miscibility test. The observation of the mixing area between the N*-LC and a cholesteryl oleyl carbonate as a standard LC was carried out through polarized optical microscope (POM). The mixing area was continuous from 0 to 15 °C. However, from 20 to 25 °C, there appeared a discontinuous boundary (a *Schlieren* texture characteristic of nematic LC) between the N*-LC and the standard LC.

	0 °C ⟵ 16 °C ⟶ 30 °C		
Screwed direction of N*-LC with D-1 (**System 1**)	↷	↷	↷
Screwed direction of N*-LC with D-3 (**System 2**)	↶	↶	↶
Screwed direction of N*-LC with both D-1 and D-3 (**System 3**)	↶	–	↷

Figure 11. Schematic representation of helical inversion of N*-LC including both D-1 and D-3 (system 3). The arrows represent the screw directions of the N*-LCs, and the sizes of the arrows represent the degree of the twisting powers of the chiral dopants.

Conclusion

We succeeded in preparation of helical pitch and helical sense-controllable chiral nematic liquid crystals (N*-LCs), by using the newly synthesized two types of chiral compounds, D-1 and D-2−D-5. Therein, D-1 is an asymmetric center-containing chiral compound, and D-2−D-5 are so-called "double chiral" compounds consisting of axially chiral binaphthyl moiety and the asymmetric center moieties, linked with methylene spacers. We found that the N*-LC including D-1 (system 1) showed an opposite temperature dependence in helical twisting power to those of the N*-LCs including D-2−D-5. Especially, the chiral dopant D-3, where both the binaphthyl moiety and the asymmetric center have the (*S*)-configuration, was highly effective for generating the N*-LC with an extraordinarily large temperature dependence. It was elucidated that the N*-LC including the two chiral dopants of D-1 and D-3 (system 3) exhibited a temperature-dependent helical inversion. The changes in helical sense and helical pitch in the N*-LC were thermally reversible. The helical pitch-controllable N*-LC (system 2) enabled us to control the screw structure as well as the spiral morphology of the helical polyacetylene by changing only the polymerization temperature. It is further expected that the helical sense-controllable N*-LC (system 3) would serve as the advanced asymmetric reaction field which makes it possible to control the screwed direction of conjugated and nonconjugated polymers through the change of the polymerization temperature.

Acknowledgment. This work was supported by a Grant-in-Aid for Science Research in a Priority Area "Super-Hierarchical Structures" (No. 446) from the Ministry of Education, Culture, Sports, Science and Technology, Japan, and also by Iketani Science and Technology Foundation.

Supporting Information Available: Figures showing ^{1}H NMR and ^{13}C NMR of all compounds and SEM photographs of helical polyacetylene synthesized in N*-LC with D-3 (system 2) at 0 and 20 °C. This material is available free of charge via the Internet at http://pubs.acs.org.

References and Notes

(1) (a) Akagi, K.; Piao, G.; Kaneko, S.; Sakamaki, K.; Shirakawa, H.; Kyotani, M. *Science* **1998**, *282*, 1683. (b) Akagi, K.; Piao, G.; Kaneko, S.; Higuchi, I.; Shirakawa, H.; Kyotani, M. *Synth. Met.* **1999**, *102*, 1406. (c) Akagi, K.; Guo, S.; Mori, T.; Goh, M.; Piao, G.; Kyotani, M. *J. Am. Chem. Soc.* **2005**, *127*, 14647. (d) Goh, M. J.; Kyotani, M.; Akagi, K. *Curr. Appl. Phys.* **2006**, *6*, 948.

(2) (a) Kang, S. W.; Jin, S. H.; Chien, L. C.; Sprunt, S. *Adv. Funct. Mater.* **2004**, *14*, 329. (b) Goto, H.; Akagi, K. *Angew. Chem., Int. Ed.* **2005**, *44*, 4322. (c) Goto, H.; Akagi, K. *Macromolecules* **2005**, *38*, 1091. (d) Goto, H.; Nomura, N.; Akagi, K. *J. Polym. Sci., Part A: Polym. Chem.* **2005**, *43*, 4298. (e) Goto, H.; Jeong, Y. S.; Akagi, K. *Macromol. Rapid Commun.* **2005**, *26*, 164. (f) Goto, H.; Akagi, K. *Chem. Mater.* **2006**, *18*, 255. (g) Goto, H.; Akagi, K. *J. Polym. Sci., Part A: Polym. Chem.* **2006**, *44*, 1042.

(3) Gottarelli, G.; Mariani, P.; Spada, G. P.; Samori, B.; Forni, A.; Solladie, G.; Hibert, M. *Tetrahedron* **1983**, *39*, 1337.

(4) Substituents of sufficiently long alkyl groups and functional groups into the side chains of the conjugated polymers gave rise to solubility and fusibility, and even liquid crystallinity and peculiar conformations such as helical structures. For example, see: (a) Oh, S. Y.; Akagi, K.; Shirakawa, H.; Araya, K. *Macromolecules* **1993**, *26*, 6203. (b) Jin, S. H.; Choi, S. J.; Ahn, W.; Cho, H. N.; Choi, S. K. *Macromolecules* **1993**, *26*, 1487. (c) Yashima, E.; Matsushima, T.; Okamoto, Y. *J. Am. Chem. Soc.* **1997**, *119*, 6345. (d) Aoki, T.; Kobayashi, Y.; Kaneko, T.; Oikawa, E.; Yamamura, Y.; Fujita, Y.; Teraguchi, M.; Nomura, R.; Masuda, T. *Macromolecules* **1999**, *32*, 79. (e) Kong, X. X.; Lam, J. W. Y.; Tang, B. Z. *Macromolecules* **1999**, *32*, 1722. (f) Lam, J. W. Y.; Tang, B. Z. *J. Polym. Sci., Part A: Polym. Chem.* **2003**, *41*, 2607. (g) Lam, J. W. Y.; Tang, B. Z. *Acc. Chem. Res.* **2005**, *38*, 745. (h) Akagi, K. *Bull. Chem. Soc. Jpn.* **2007**, *80*, 649.

(5) For instance: Shirakawa, H.; Masuda, T.; Takeda, T. In *The Chemistry of Triple-Bonded Functional Groups*, Suppl. C2; Patai, S., Ed.; Wiley: Chichester, U.K., 1994; Vol. 2, Chapter 17.

(6) (a) Finkelmann, H.; Stegemeger, H. *Z. Naturforsch., A: Phys. Sci.* **1973**, *28*, 799. (b) Heppke, G.; Lötzsch, D.; Oestreicher, F. *Naturforsch., A: Phys. Sci.* **1987**, *42*, 279. (c) Dierking, I.; Giesselmann, F.; Zugemaier, P.; Kuczynski, W.; Lagerwall, S. T.; Stebler, B. *Liq. Cryst.* **1993**, *3*, 399. (d) Mitov, M.; Dessaud, N. *Nat. Mater.* **2006**, *5*, 361.

(7) Sackmann, E.; Meiboom, S.; Snyder, L. C.; Meixner, A. E.; Dietz, R. E. *J. Am. Chem. Soc.* **1968**, *9*, 3567.

(8) (a) Baessler, H.; Labes, M. M. *J. Chem. Phys.* **1970**, *52*, 631. (b) Baessler, H.; Malya, P. A. G.; Nes, W. R.; Labes, M. M. *Mol. Cryst. Liq. Cryst.* **1970**, *6*, 329.

(9) (a) Stegemeyer, H.; Siemensmeyer, K. *Naturforsch., A: Phys. Sci.* **1989**, *44*, 1127. (b) Dierking, I.; Giesselmann, F.; Zugemaier, P.; Mohr, K.; Zaschke, H.; Kuczynski, W. *Z. Naturforsch.* **1994**, *49a*, 1081.

(10) (a) Slaney, A. J.; Nishiyama, I.; Styring, P.; Goodby, J. W. *J. Mater. Chem.* **1992**, *2*, 805. (b) Kuball, H. -G.; Muller, T.; Weyland, H. -G. *Mol. Cryst. Liq. Cryst.* **1992**, *215*, 271. (c) Styring, P.; Vuijk, J. D.; Nishiyama, I.; Slaney, A. J.; Goodby, J. W. *J. Mater. Chem.* **1993**, *2*, 399.

(11) Kanazawa, K.; Higuchi, I.; Akagi, K. *Mol. Cryst. Liq. Cryst.* **2001**, *364*, 825.

(12) (a) Solladie, G.; Zimmermann, R. *Angew. Chem., Int. Ed.* **1984**, *23*, 348. (b) Gottarelli, G.; Spada, G. P.; Bartsch, R.; Solladie, G.; Zimmermann, R. *J. Org. Chem.* **1986**, *51*, 589. (c) Bhatt, J. C.; Keast, S. S.; Neubert, M. E.; Petschek, R. C. *Liq. Cryst.* **1995**, *18*, 367.

(13) (a) Akagi, K.; Higuchi, I.; Piao, G.; Shirakawa, H.; Kyotani, M. *Mol. Cryst. Liq. Cryst.* **1999**, *332*, 463. (b) Piao, G.; Akagi, K.; Shirakawa, H.; Kyotani, M. *Curr. Appl. Phys.* **2001**, *1*, 121.

(14) Emoto, N.; Saito, H.; Furukawa, K.; Inukai, T. *Proc. Jpn. Display* **1986**, *86*, 286.

(15) (a) Rokunohe, J.; Yoshizawa, A. *J. Mater. Chem.* **2005**, *15*, 275. (b) Yoshizawa, A.; Sato, M.; Rokenohe, J. *J. Mater. Chem.* **2005**, *15*, 3285.

(16) (a) Grandjean, F. *C. R. Acad. Sci.* **1921**, 172. (b) Cano, R. *Bull. Soc. Fr. Mineral.* **1968**, *91*, 20. (c) Gottarelli, G.; Samori, B.; Stremmenos, C.; Torre, G. *Tetrahedron* **1981**, *37*, 395.

(17) Finkelmann, H.; Stegemeger, H. *Ber. Bunsen-Ges. Phys. Chem.* **1978**, *82*, 1302.

MA0703655